# A Kinetic Description of Diffusion-Controlled Intramolecular Excimer and Exciplex Formation

**Guojun Liu and J. E. Guillet***

*Department of Chemistry, University of Toronto, Toronto, Ontario, Canada M5S 1A1*

*Received July 20, 1989; Revised Manuscript Received February 23, 1990*

ABSTRACT: A new scheme is proposed for diffusion-controlled excimer formation between polymer chain ends. Unlike the Birks scheme,[1] the new scheme makes no use of rate expressions for excimer formation and dissociation. Instead, excimer formation is described as the natural consequence of chain end diffusion. Computer simulation based on the new scheme yields monomer and excimer decay curves similar to the ones experimentally observed. When used for intramolecular excimer formation kinetics, a convenient and sensitive method can be developed from this theory for measuring the diffusion coefficients, $D$, of polymer ends, the free energy, $\epsilon_0$, for excimer formation, root-mean-square end-to-end distances, $R_n$, of polymer chains, and fluorescence lifetimes of excimers, $\tau_D$.

## I. Introduction

The kinetics of excimer and exciplex formation has previously been described by the well-known Birks scheme:[1]

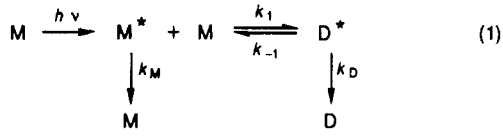


(1)

where $k_M$ and $k_D$ are rate constants for self-deactivation processes of the excited monomer M* and excimer D*; $k_1$ and $k_{-1}$ are rate constants for the interchange reactions between M* and D*.

The above scheme has been widely used to describe both intermolecular[2,4] and intramolecular[5,6] excimer or exciplex formation. When used to describe excimer formation between two reactive groups connected by a long polymer chain undergoing Brownian motion, the intramolecular rate constant $k_1$ can be calculated for different polymeric dynamic models using the general theory for diffusion-controlled reactions first proposed by Wilemski and Fixman[7-9] and subsequently modified by others.[10-18] According to Wilemski and Fixman,[7-9] rates of reactions between end groups of a polymer chain can be depicted as the rate at which one end of a polymer chain enters a sink, such as a reaction sphere of radius $R_a$, selected around the other end group. The rate constant $k_1$ has been found to be time-dependent. At very short times, the reaction is controlled by the intrinsic rate $kC_0$, where $k$ is the intrinsic second-order rate constant and $C_0$ is the equilibrium sink concentration, the portion of polymer chains that possess the configurations enabling the end groups to react at time $t = 0$.[18] In the long-time limit ($t \rightarrow \infty$), the reaction can be described by a uniquely defined rate constant $k_1(t\rightarrow\infty)$ that is independent of $k$, the intrinsic second-order rate constant, if the reaction is diffusion-controlled.[18] Rather, $1/k_1(t\rightarrow\infty)$ is characteristic of the longest relaxation time of the polymer chain that connects the reactive groups. In the intermediate times, $k_1(t)$ has a complicated time dependence.[18]

In fortunate cases, $k_1(t)$ in certain systems actually reaches its asymptotic value $k_1(t\rightarrow\infty)$ very rapidly ($\sim$1 ns) and the experimental determination of $k_1(t\rightarrow\infty)$ by studying excimer formation reactions between groups attached to polymer chain ends has been possible.[19-21] These studies greatly contributed to the understanding of the dynamic behavior of polymer chains.

However, the general use of the Birks scheme in describing intramolecular excimer formation has a few disadvantages. (1) $k_1(t)$ do not necessarily reach their asymptotic values fast enough in the time domain in which the experiment is performed. (2) It makes unnecessary use of rate equations. The reaction of excimer formation is diffusion-controlled, and it is sufficient to describe the process by diffusion equations. Due to the unnecessary use of rate laws, time-dependent rate constants arise sometimes that are in contradiction to the conventional definition of a constant. (3) The kinetic description of the system becomes unnecessarily complex when one introduces the time-dependent rate constant $k_1(t)$.[22]

This paper presents a simple and straightforward scheme for describing intramolecular excimer formation kinetics. In this approach, no rate equations will be used for describing excimer formation and dissociation. Since excimer formation is assumed to be diffusion-controlled, excimer formation is described as arising from the natural diffusion motion of the chain ends.

## II. Theory

**Excimer or Exciplex.** A molecule M in an electronically excited state M* may be a very polarizable species and interacts with other polar or polarizable species. If M* interacts with M and forms a collision complex D* that is more stable than M* + M, D* is called an excimer. If M* forms a collision complex with a different molecule N, the complex formed is called an exciplex.[23] Diffusion and kinetic equations are developed below for the system based on a discussion of excimer formation. The equations are equally applicable to exciplex formation kinetics, provided that there are no accompanying electron-transfer processes.

The interaction between M* and M is orientation- and distance-dependent. For planar molecules such as pyrene (Py), parallel pairs of Py and Py* with overlapping center axes are energetically more favorable orientations.[24] Since the relative rotational motion between M* and M is, in general, much faster than the relative diffusional motion between them,[25] it can be assumed that most of these M* and M pairs that are brought together by the relative diffusion between them are in the energetically more favorable parallel orientations with center axes of M* and M overlapping. For pyrene molecules, Py* and Py, approaching one another in the parallel fashion, the attractive part of the interaction potential has been shown to be inversely proportional to the third power of the in-

0024-9297/90/2223-4292$02.50/0 © 1990 American Chemical Society

terplanar separation distance,[1] or

$$U_A(r) \propto 1/r^3 \quad (2)$$

In this paper, kinetic equations for excimer formation are derived assuming that the interaction potential between M* and M is described by the Lennard-Jones equation:[26]

$$U(r) = -\epsilon_0[2(r_0/r)^6 - (r_0/r)^{12}] \quad (3)$$

The methodology can, however, be applied equally effectively when different interaction potentials are assumed between M* and M. The validity of different interaction potentials can be judged from the agreement between kinetic curves theoretically predicted and those obtained experimentally.

In light of the Lennard-Jones interaction potential, the interaction energy between M* and M approaches zero when the two species are separated by infinite distances and $-\epsilon_0$ when they are separated by a distance $r_0$. For this system, we define the following. If the two interacting species are separated by a distance $r_0$, they form a perfect excimer; if they are infinitely apart, they are a perfect monomer pair M* + M; and if they are separated by any intermediate distances, they are intermediates between a monomer pair M* + M and an excimer. Suppose that M* and M are separated by $r$. The extent of excimer formation is quantified by

$$X(r) = 2(r_0/r)^6 - (r_0/r)^{12} \qquad r \geq r_0 \quad (4)$$

because the stabilization energy for this monomer pair is $X(r)\epsilon_0$. The extent of monomer behavior is given by $1 - X(r)$. We set the excimer self-deactivation rate constant to be $k_D = 1/\tau_D$ and that for the monomer pair to be $k_M = 1/\tau_M$, where $\tau_D$ and $\tau_M$ are fluorescence lifetimes of excimers and monomers, respectively.

When the separation distance between M* and M is smaller than $r_0$ (~4 Å for pyrene),[23] we further assume that the monomeric pair M + M* behaves as a typical excimer and self-deactivates with rate constant $k_D$. This definition is questionable, especially when $r$ is smaller than $r_0/(2^{1/6})$, after which the interactive potential is repulsive according to eq 3. We do not need to worry, however, about the arbitrariness in the definition in this $r$ range due to the small probability of finding a monomeric pair M* and M to be separated by an distance shorter than $r_0/(2^{1/6})$.

**Diffusion Equation for Chromophore Pairs Attached to Polymer Chain Ends.** In this case, we will study the kinetics in Θ-solvents and assume that the chromophore end groups are not interactive in the ground state. By further assuming that polymer chains are long enough so that chain conformations are not perturbed by the introduction of the chromophore end groups, the end-to-end distance distribution function is then described by the Gaussian form $G(r)$ at time zero.

At time zero, a δ-pulse of radiation excites one end chromophore of a polymer chain. M* interacts with the other end chromophore and may form an excimer. The interaction energy between the chromophore end groups has been assumed to be given by Lennard-Jones interaction potential $U(r)$. It is further assumed that if enough time is allowed for the system to relax, the new equilibrium end-to-end distance distribution $P(r)$ of a Gaussian chain bearing a pair of interacting monomer pairs M* and M is a Gaussian form modified by a Boltzmann energy correction factor:

$$P(r) = \gamma^{-1}G(r)\exp[-U(r)/kT]$$
$$= \gamma^{-1}G(r)\exp[(\epsilon_0/kT)[2(r_0/r)^6 - (r_0/r)^{12}]] \quad (5)$$

where $kT$ is the thermal energy. $\gamma^{-1}$, a normalization factor, is given by

$$\gamma = \int_0^\infty G(r)e^{-U(r)/kT}\,dr \quad (6)$$

for a chain of infinite length. The δ-pulse shifts the system from the old equilibrium state to a new equilibrium state.

The change in system properties due to an outside perturbation can be described by response theory.[27] We are interested in the variation of the end-to-end distance distribution function of the system with time. The time-dependent end-to-end distance distribution function can also be obtained from the generalized diffusion operator approach introduced by Kirkwood.[28] Neglecting hydrodynamic interactions between polymer segments,[28] an earlier technique using probability theory[29] can be used for the derivation of the diffusion equation. One first ignores the self-deactivation of excimers D* and excited monomers M*, and the system is assumed to have sufficient time to relax from one equilibrium state to the other. Before the δ-pulse excitation, the relative diffusion is governed by a Gaussian end-to-end distance probability distribution function. After the δ-pulse excitation, the relative diffusion of the ends is governed by the end-to-end distance probability distribution function given by eq 5. Following the procedures described by Liu and Guillet,[29] we picture the relative diffusion of the end groups as being comprised of many small jumps of distance δ occurring with very high frequency $\psi$. In spherical coordinates, one end of a polymer chain is taken to be fixed at the origin. The relative change in the end-to-end distance of a chain is visualized to be caused by jumps of the other end in space. Since we are interested in distance changes between the end groups, only the radial component $\delta_r$ of jump distance δ must be considered. It has been shown that[29]

$$\delta_r^2 = (1/3)\delta^2 \quad (7)$$

Denoting the probability of finding the moving end to be $r$ distance away from the origin at time $t + 1/\psi$ as $S(r,t+1/\psi)$, the difference equation for $S(r,t+1/\psi)$ is[29]

$$S(r,t+1/\psi) = \rho(r+\delta_r\rightarrow r)S(r+\delta_r,t) + \rho(r-\delta_r\rightarrow r)S(r-\delta_r,t) + [1 - \rho(r\rightarrow r-\delta_r) - \rho(r\rightarrow r+\delta_r)]S(r,t) \quad (8)$$

where $\rho(r+\delta_r\rightarrow r)$ and $\rho(r-\delta_r\rightarrow r)$ are the probabilities that the moving end of a chain that has an end-to-end distance of $r + \delta_r$ or $r - \delta_r$ will make a jump and move to a position with an end-to-end distance of $r$; $\rho(r\rightarrow r-\delta_r)$ and $\rho(r\rightarrow r+\delta_r)$ are the probabilities that the moving end of a chain that has an end-to-end distance of $r$ will make a jump and move to a position with an end-to-end distance of $r + \delta_r$ or $r - \delta_r$; $S(r+\delta_r,t)$, $S(r,t)$, and $S(r-\delta_r,t)$ are the probabilities of finding the moving end to be $r + \delta_r$, $r$, and $r - \delta_r$ distances away from the origin at time $t$. Following the same procedure used by Liu and Guillet,[29] the expressions for $\rho(r+\delta_r\rightarrow r)$ and $\rho(r-\delta_r\rightarrow r)$ have been shown to be

$$\rho(r+\delta_r\rightarrow r) = \rho(r\rightarrow r-\delta_r) + (\delta_r^2/4)[[2/r^2 + 3/R_n^2] - (\epsilon/r^2)[84(r_0/r)^6 - 156(r_0/r)^{12}]] + O(\delta_r^3) \quad (9)$$

and

$$\rho(r-\delta_r\rightarrow r) = \rho(r\rightarrow r+\delta_r) + (\delta_r^2/4)[[2/r^2 + 3/R_n^2] - (\epsilon/r^2)[84(r_0/r)^6 - 156(r_0/r)^{12}]] + O(\delta_r^3) \quad (10)$$

where $\epsilon$ is given by

$$\epsilon = \epsilon_0/kT \tag{11}$$

where $kT$ is the thermal energy, $O(\delta_r^3)$ means that terms containing $\delta_r$ of order 3 or higher have been omitted, and $R_n$ is the root-mean-square end-to-end distance of the polymer chain. The expressions for $\rho(r\rightarrow r+\delta_r)$ and $\rho(r\rightarrow r-\delta_r)$ have also been evaluated following the procedure previously described[29] and are found to be

$$\rho(r\rightarrow r+\delta_r) = 1/2 + (\delta_r/4)[(2/r - 3r/R_n^2) - (12\epsilon/r)[(r_0/r)^6 - (r_0/r)^{12}]] + O(\delta_r^2) \tag{12}$$

and

$$\rho(r\rightarrow r-\delta_r) = 1/2 - (\delta_r/4)[(2/r - 3r/R_n^2) - (12\epsilon/r)[(r_0/r)^6 - (r_0/r)^{12}]] - O(\delta_r^2) \tag{13}$$

Expanding $S(r,t+1/\psi)$ in eq 8 in Taylor's series, truncating after the term containing $1/\psi$ and expanding $S(r+\delta_r,t)$ and $S(r-\delta_r,t)$, truncating after the second-order terms of $\delta_r^2$, and inserting eqs 9, 10, 12, and 13 yield

$$\frac{\partial S(r,t)}{\partial t} = D\left[\frac{\partial^2 S(r,t)}{\partial r^2} - [(2/r - 3r/R_n^2) - (12\epsilon/r)[(r_0/r)^6 - (r_0/r)^{12}]]\frac{\partial S(r,t)}{\partial r} + [[2/r^2 + 3/R_n^2] - (\epsilon/r^2)[84(r_0/r)^6 - 156(r_0/r)^{12}]]S(r,t)\right] \tag{14}$$

where $D$ is the coefficient of relative diffusion between the polymer end groups and is defined by

$$D = \psi\delta_r^2/2 \tag{15}$$

according to Liu and Guillet.[29]

Equation 14 is a diffusion equation for the end groups of polymer chains labeled with monomeric chromophores M* and M in a differential form. The equation can be solved with the use of the following initial and boundary conditions:

$$S(r,0) = G'(r) \tag{16}$$

$$S(0,t) = 0 \tag{17}$$

$$S(r>m_x,t) = 0 \tag{18}$$

where $m_x$ is the contour length of the polymer chain and $G'(r)$ is a modified Gaussian end-to-end distance distribution function. By definition

$$\int_0^{M_x} G'(r)\,dr = 1 \tag{19}$$

and

$$G'(r) = G(r)/\int_0^{M_x} G(r)\,dr \tag{20}$$

where $G(r)$ is a Gaussian end-to-end distance distribution for a chain of infinite length and a root-mean-square end-to-end distance of $R_n$, or

$$G(r) = 4\pi r^2\left[\frac{3}{2\pi R_n^2}\right]^{3/2}\exp[-(3/2)(r/R_n)^2] \tag{21}$$

The difference between $G'(r)$ and $G(r)$ is negligible when $m_x/R_n$ is greater than 3. The reason is clear from studying eq 21. As $r$ increases, $G(r)$ decreases exponentially with the square of $r$. It is easy to show that the probability density function $G(r)$ has negligible readings if $r$ is greater than $3R_n$.

**Monomer and Excimer Fluorescence Decay Kinetics.** In this section, we incorporate the sink terms caused by self-deactivation processes of excimer D* and monomers M* following the procedure described previously.[30] In this new context, $S(r,t)$ is the probability of finding the end groups still in the excited state either as M* or D* at time $t$. The extent of the excimer feature is defined by the separation distance between the end groups and quantified by eq 4. The differential equation for $S(r,t)$ of the system is

$$\frac{\partial S(r,t)}{\partial t} = D\left[\frac{\partial^2 S(r,t)}{\partial r^2} - [(2/r - 3r/R_n^2) - (12\epsilon/r)[(r_0/r)^6 - (r_0/r)^{12}]]\frac{\partial S(r,t)}{\partial r} + [[2/r^2 + 3/R_n^2] - (\epsilon/r^2)[84(r_0/r)^6 - 156(r_0/r)^{12}]]S(r,t)\right] - \frac{X(r)S(r,t)}{\tau_D} - \frac{[1 - X(r)]S(r,t)}{\tau_M} \tag{22}$$

where $\tau_D$ and $\tau_M$ are the fluorescence lifetimes of a perfect excimer D* and a perfect monomer M*, respectively. The initial and boundary conditions for the differential equation are the same as those required by eq 14.

$S(r,t)$ can be solved from eq 22 numerically following the previous procedure.[30] The probability of finding excimers in the system at time $t$ is given by

$$S_D(t) = \int_{r_0}^{m_x} X(r)S(r,t)\,dr + \int_{r_0/(2^{1/6})}^{r_0} S(r,t)\,dr \tag{23}$$

The probability of finding a monomer in the system at time $t$ is

$$S_M(t) = \int_{r_0}^{m_x} [1 - X(r)]S(r,t)\,dr \tag{24}$$

Since $S_D(t)$ and $S_M(t)$ are proportional to excimer and monomer emission intensities at time $t$, plotting $S_D(t)$ and $S_M(t)$ versus time $t$ yields transient excimer and monomer emission intensity curves.

## III. Experimental Section

All numerical solutions were performed on an Apollo computer. A numerical solution for $S(r,t)$ using eq 14 requires that the contour length of a polymer chain be divided into numerous distance intervals, and the computation is therefore extremely time-consuming. The small distance increment required for performing the computation is caused by the approximations made in deriving eq 14 from the more general diffusion equation given by eq 8. The probability of making a jump from a position with an end-to-end distance of $r$ to a position with an end-to-end distance of $r + \delta_r$ was approximated by eq 12. The terms containing $\delta_r^2$ and terms containing $\delta_r$ of even higher orders have been omitted. The truncation is valid only if the second term on the right-hand side of eq 12 is much smaller than $^1/_2$. It can be shown that the condition is satisfied at small $r$ values only if very small $\delta_r$ values are used. Instead of solving eq 14, we used eq 8 and the exact expressions[29] of $\rho(r+\delta_r\rightarrow r)$, $\rho(r-\delta_r\rightarrow r)$, $\rho(r\rightarrow r+\delta_r)$, and $\rho(r\rightarrow r-\delta_r)$ for $S(r,t)$. For all simulations, the $\delta_r$ value is typically assumed to be 0.1 Å.

The kinetic equation given by eq 22 is time-consuming to solve numerically. The more general kinetic equation

is

$$S(r,t+1/\psi) = \rho(r+\delta_r \rightarrow r)\left[1 - \frac{X(r+\delta_r)}{\tau_D\psi} - \frac{1-X(r+\delta_r)}{\tau_M\psi}\right]S(r+\delta_r,t) + \rho(r-\delta_r \rightarrow r)\left[1 - \frac{X(r-\delta_r)}{\tau_D\psi} - \frac{1-X(r-\delta_r)}{\tau_M\psi}\right]S(r-\delta_r,t) + [1 - \rho(r \rightarrow r+\delta_r) - \rho(r \rightarrow r-\delta_r)]\left[1 - \frac{X(r)}{\tau_D\psi} - \frac{1-X(r)}{\tau_M\psi}\right]S(r,t) \quad (25)$$

where $\psi$ is the jump frequency of the chain end which is related to diffusion coefficient $D$ by eq 15. After $S(r,t)$ values are obtained numerically from eq 25, the probability of finding an excimer or a monomer in the system is computed by using eqs 23 and 24.

## IV. Results and Discussion

In cases when $k_1(t)$ approach their asymptotic values so rapidly that $k_1(t)$ can be assumed to be time-independent, the Birks scheme predicts that monomer emission should decay as a sum of two exponential components:

$$S_m(t) = A_1e^{-\lambda_1 t} + A_2e^{-\lambda_2 t} \quad (26)$$

where $A_1$, $A_2$, $\lambda_1$, and $\lambda_2$ are complex functions of $k_1$, $k_{-1}$, $k_m$, and $k_D$. Under the same conditions, the excimer emission $S_D(t)$ should grow in and decay as the difference of two exponential terms with the same rate constants $\lambda_1$ and $\lambda_2$:

$$S_D(t) = A_3(e^{-\lambda_1 t} - e^{-\lambda_2 t}) \qquad \lambda_1 < \lambda_2 \quad (27)$$

where $A_3$ is a constant. In cases where the time dependence of rate constant $k_1(t)$ needs to be taken into account, kinetic equations become more complicated. The same qualitative behavior, that monomer emission decays consistently with increasing time and excimer emission grows in and decays with time, is, however, observed. All kinetic curves generated from our model agree with this basic trend. The detailed differences between results obtained from our approach and those of the Birks scheme will be examined in a subsequent paper.

**Equilibrium End-to-End Distance Distribution Function for Chains Bearing Interactive Monomeric Pairs.** As discussed previously, if the excitation energy of monomer M* and excimer D* survives for a sufficiently long time after the $\delta$-pulse, the interaction between the end groups M* and M will shift the system to a new equilibrium. The end-to-end distance distribution function for the system at the new equilibrium is given by eq 5. The equilibrium end-to-end distance distribution function for a hypothetical chain possessing a contour length of 200 Å (corresponding to ca. 160 C–C bonds) and a root-mean-square end-to-end distance of 50 Å is illustrated in Figure 1. Parameters needed for describing the interactions between the end groups are assumed to be $r_0 = 4.0$ Å and $\epsilon_0/kT = 7.0$. At equilibrium, the probability of finding that the ends of a chain exist as an excimer is computed to be 21.5%. Equilibrium probabilities for excimer formation using different $\epsilon_0/kT$ parameters are summarized in Table I.

**Diffusion Behavior of Chromophore Pairs Attached to Polymer Chain Ends.** In Figure 2, the end-to-end distance distribution functions of a polymer chain after different numbers of jump steps are shown. The following parameters are used for performing the simulation. $R_n$, the root-mean-square end-to-end distance of the polymer chain, is arbitrarily assumed to be 25 Å; $m_x$, the contour length of the chain, is assumed to be 70 Å (corresponding to ca. 50 C–C bonds); $\delta_r$, the average distance change along the radial direction achieved by each jump, is assumed to be 0.1 Å; $\epsilon_0/kT$, the energy parameter appearing in eq 3, is assumed to be 3; and $r_0$ in eq 3 is assumed to be 4 Å. In the simulations, chains of short contour length are assumed because of their time-saving feature. As the number of jumps made by the moving chain end increases, the Gaussian end-to-end distance distribution function at time $t = 0$ changes and eventually approaches the end-to-end distance distribution function given by eq 5.

The number of jumps the moving end has made, $n$, is related to chain end diffusion time $t$ by the following relation:

$$2Dt = n\delta_r^2 \quad (28)$$

where $D$ is the coefficient of relative diffusion between the

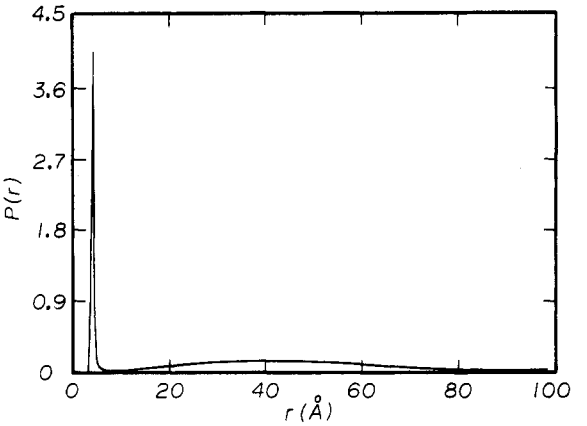


**Figure 1.** An end-to-end distance distribution function computed with eq 5: $R_n = 50$ Å, $m_x = 200$ Å, $r_0 = 4.0$ Å, and $\epsilon_0/kT = 7$.

**Table I**
**Probability of Finding Excimers in an Equilibrium System Characterized by an End-to-End Distance Distribution Function Given by Eq 5[a]**

| $\epsilon_0/kT$ | $S_D$, % | $\epsilon_0/kT$ | $S_D$, % |
|---|---|---|---|
| 4.0 | 1.96 | 8.0 | 40.0 |
| 5.0 | 4.46 | 9.0 | 61.5 |
| 6.0 | 10.1 | 10.0 | 78.3 |
| 7.0 | 21.5 | | |

[a] The Gaussian chain has been assumed to have a root-mean-square end-to-end distance of 50 Å and a contour length of 200 Å. The distance $r_0$ at which excimer forms has been assumed to be 4.0 Å.

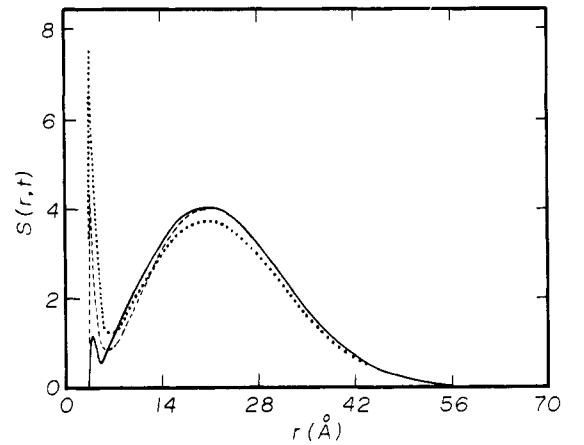


**Figure 2.** Time evolution of end-to-end distance distribution function: (—) after 100 jumps; (– – –) after 4000 jumps; (···) after 40 000 jumps.

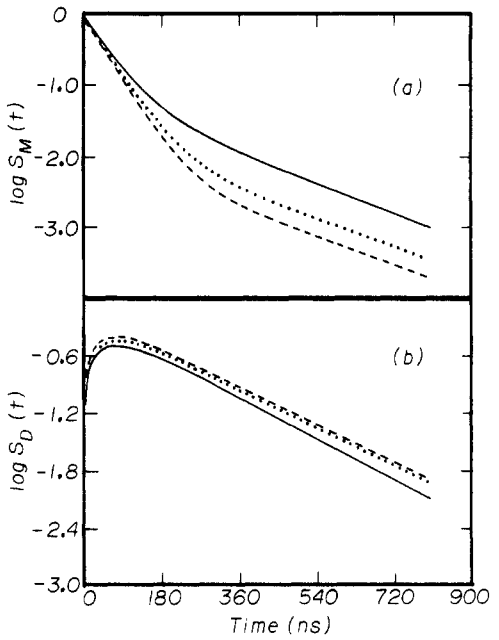


**Figure 3.** Effect of end-group interaction on monomer and excimer fluorescence decay curves. The chain is assumed to possess $R_n$ = 25 Å, $m_x$ = 70 Å, $\tau_M$ = 100 ns, $\tau_D$ = 200 ns, $r_0$ = 4.0 Å, and $D = 5.0 \times 10^{-7}$ cm²/s. (a) Monomer decay profiles: (—) $\epsilon_0/kT$ = 9; (···) $\epsilon_0/kT$ = 15; (– – –) $\epsilon_0/kT$ = 25. (b) Transient excimer fluorescence intensity profiles.

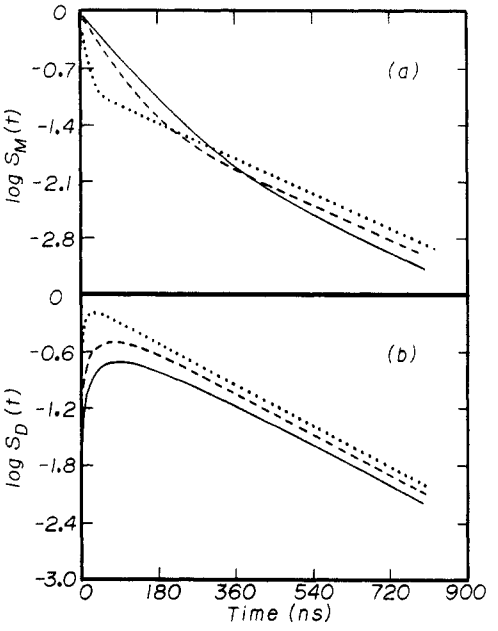


**Figure 4.** Effect of end-group diffusion on monomer and excimer fluorescence decay curves. The chain is assumed to possess $R_n$ = 25 Å, $m_x$ = 70 Å, $\tau_M$ = 100 ns, $\tau_D$ = 200 ns, $r_0$ = 4.0 Å, and $\epsilon_0/kT$ = 9. (a) Monomer decay profiles: (—) $D = 2.0 \times 10^{-7}$ cm²/s; (– – –) $D = 5.0 \times 10^{-7}$ cm²/s; (···) $D = 4.0 \times 10^{-6}$ cm²/s. (b) Transient excimer fluorescence intensity profiles.

chain ends and $\delta_r$ is the average distance change along the radial direction achieved by each jump. If a diffusion coefficient of $1.0 \times 10^{-6}$ cm²/s, close to that obtained by Xu[31] for chains of such length, is assumed for our case, the $n$ value of 40 000 corresponds to a $t$ value of 20 ns. The system reaches monomer–excimer distribution equilibrium fairly rapidly.

**Effect of End-Group Interaction.** Figure 3 shows a set of transient fluorescence intensity profiles obtained numerically for monomer and excimer emissions by assuming various interaction energy parameters. The hypothetical chain bearing the fluorescent end groups is assumed to possess a root-mean-square end-to-end distance, $R_n$, of 25 Å and a contour length, $m_x$, of 70 Å. For these calculations lifetimes of monomer and excimer emissions are arbitrarily assumed to be 100 and 200 ns, respectively. Birks[1] reports $\tau_M$ and $\tau_D$ values for a number of aromatic chromophores. In polar solvents such as 95% ethanol, the $\tau_D$ values for excimers are ca. 2–3 times that of monomer emission. In nonpolar solvents, the naphthalene excimer has almost the same lifetime as the monomer (~100 ns). On the other hand, the pyrene excimer in cyclohexane has a $\tau_D$ value of 65 ns as compared to $\tau_M$ of 450 ns. This compares well with data on pyrene end-capped polystyrene reported by Winnik et al.[6] for which $\tau_D$ = 58 ns and $\tau_M$ = 242 ns. The effect of particular choices for $\tau_M$ and $\tau_D$ will be discussed later. Finally, the $r_0$ value in eq 3 is assumed to be 4.0 Å and the coefficient of relative diffusion between the chain ends is assumed to be $5.0 \times 10^{-7}$ cm²/s.

Plotting log $S_M(t)$ versus time $t$ does not yield linear curves (Figure 3a) because at short times, monomer is consumed by self-decay and conversion to excimer. As time progresses, an equilibrium excimer-to-monomer concentration ratio is reached. Since the monomer decays with a larger rate constant, at long times, it is expected that excimers will dissociate back to monomers, and the log $S_M(t)$ vs $t$ plot is curved.

As the interaction energy parameter $\epsilon_0/kT$ increases, the maximum curvature in log $S_M(t)$ vs $t$ plot occurs at a smaller log $S_M(t)$ value. This is as expected. The larger the $\epsilon_0/kT$ value, the larger the equilibrium excimer-to-monomer concentration ratio.

The back-dissociation of excimer into monomer at long times can be seen from the excimer emission decay curve obtained by assuming an interaction energy parameter of $\epsilon_0/kT$ = 9. The excimer decay curves obtained by assuming interaction energy parameters of 15 and 25 are almost parallel at long times. The curve with an interaction energy parameter of 9 is obviously concave downward at long times. Both the transient emission intensity profiles of the monomer and excimer are sensitive functions of the interaction parameters assumed.

The maximum positions of the transient excimer fluorescence intensity profiles are almost unchanged by various interaction energy parameters. The maxima for the three curves all occur ca. 76 ns after the $\delta$-pulse excitation.

**Effect of End-Group Diffusion.** In Figure 4, a set of transient fluorescence intensity curves computed with different diffusion coefficients for the chain ends is shown. The modeling was performed for the same hypothetical chain as discussed above and the interaction energy parameter is assumed to be 9. As the diffusion coefficient increases, a more rapid decay is seen for monomer emission intensity at short times. As the equilibrium excimer-to-monomer concentration ratio is reached, since in this case the excimer decays more slowly than the monomer, excimers dissociate back to monomer at long times. The larger the diffusion coefficient, the more abrupt the transition from short-time decay behavior to long-time behavior. The smaller the diffusion coefficient, the later the transition occurs.

Increasing the diffusion coefficients of the chain ends shifts the maxima in transient excimer emission intensity profiles to shorter times. With a diffusion coefficient of $2.0 \times 10^{-7}$ cm²/s, the maximum occurs at 87 ns. Increasing the diffusion coefficient to $5.0 \times 10^{-7}$ cm²/s shifts the maximum to 77 ns. With a diffusion coefficient of $4.0 \times 10^{-6}$ cm²/s, the maximum is shifted to 30 ns. Thus, the

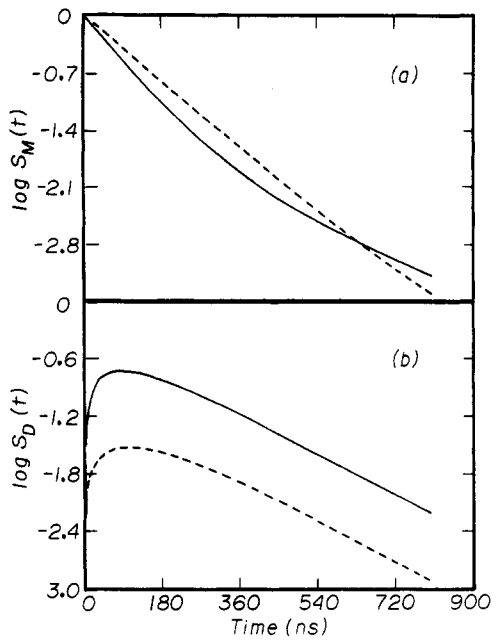


**Figure 5.** Effect of chain conformation change on monomer and excimer fluorescence decay curves. $\tau_M$ = 100 ns, $\tau_D$ = 200 ns, $r_0$ = 4.0 Å, $\epsilon_0/kT$ = 9, $D$ = 2.0 × $10^{-7}$ $cm^2/s$. (—) $R_n$ = 25 Å and $m_x$ = 70 Å. (- - -) $R_n$ = 50 Å, $m_x$ = 200 Å. (a) Monomer decay profiles. (b) Transient excimer fluorescence intensity profiles.

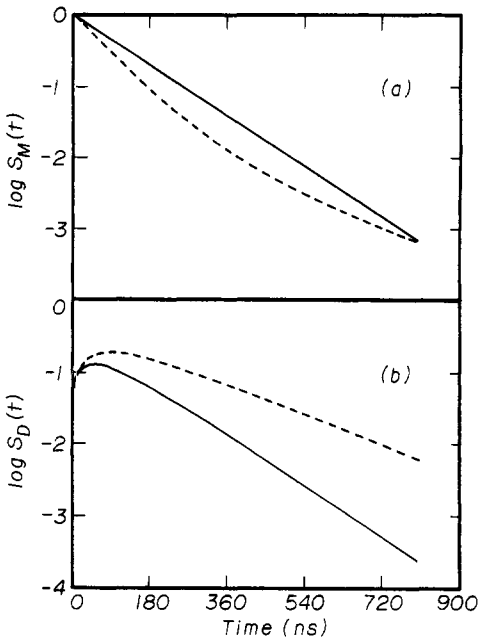


**Figure 6.** Monomer and excimer fluorescence decay curve changes caused by variation in monomer and excimer emission lifetimes. $R_n$ = 25 Å, $m_x$ = 70 Å, $r_0$ = 4.0 Å, $\epsilon_0/kT$ = 9, $D$ = 2.0 × $10^{-7}$ $cm^2/s$. (—) $\tau_M$ = 200 ns; $\tau_D$ = 50 ns. (- - -) $\tau_M$ = 100 ns; $\tau_D$ = 200 ns. (a) Monomer decay profiles. (b) Transient excimer fluorescence intensity profiles.

transient emission profiles of monomer and excimer are both sensitive functions of the diffusion coefficients of the chain ends.

**Effect of Chain Conformation Changes or Molecular Weight Changes.** In Figure 5, decay curves obtained for samples with different root-mean-square end-to-end distances are shown. In the same solvent, the root-mean-square end-to-end distances of polymer samples are different if samples of different molecular weights are used. In different solvents, the root-mean-square end-to-end distances of a polymer sample can be different due to different interactions between the polymer chains and solvents and therefore different polymer chain conformations.

As the root-mean-square end-to-end distance of the polymer sample increases, the curvature in the plot of log $S_M(t)$ vs $t$ is reduced. The explanation is twofold. First, as $R_n$ increases, the maximum in the Gaussian probability distribution profile at time $t$ = 0 is more removed from $r_0$, the distance at which excimer forms. It is, therefore, expected that as $R_n$ increases, the rapid consumption of monomers to form excimers due to diffusion at short times will be less important. Second, as $R_n$ increases, the equilibrium excimer-to-monomer concentration ratio decreases. As equilibrium excimer concentration decreases, the dissociation of excimers into monomers at long times will not increase the concentration of monomers significantly.

As before, fluorescence decay curves of the monomers are sensitive functions of the root-mean-square end-to-end distances of polymer chains.

**Effect of Changing $\tau_M$ and $\tau_D$.** In Figure 6 transient fluorescence emission intensity curves obtained by using different decay lifetimes for excimer and monomer emissions are shown. The computation was performed for the same hypothetical chain using a root-mean-square end-to-end distance of 25 Å. Again, the decay features are seen to be drastically changed by varying the fluorescence lifetime of each species.

## V. Conclusions

The model proposed makes no use of rate equations for diffusion-controlled excimer or exciplex formation. Computer modeling has demonstrated that the new model yields decay curves similar to those experimentally observed.

A new and convenient method can be developed based on this model for the experimental measurement of the following parameters: energy interaction parameter $\epsilon_0/kT$, chain end diffusion coefficient $D$, root-mean-square end-to-end distance $R_n$, and fluorescence lifetime of excimer emission $\tau_D$. Fitting monomer and excimer decay curves requires that the experiment be performed in a Θ-solvent. Once diffusion coefficients of the chain ends in Θ-solvents are known, the diffusion coefficients in non-Θ-solvents can be deduced. The model can then be further extended and used to probe the conformations of polymer chains in non-Θ-solvents.

**Acknowledgment.** We are grateful to the Natural Sciences and Engineering Research Council of Canada for financial support of this work. G.L. thanks the Education Ministry of the P.R.C. for a scholarship that made his study at the University of Toronto possible and the University of Toronto for a Connaught Scholarship and for a University of Toronto Open Fellowship. J.E.G. is grateful to the Canada Council for support in the form of a Killam Research Fellowship. Finally, we acknowledge very helpful discussions with Professor M. A. Winnik of this Department, who has pioneered the experimental studies of this field of research.

## References and Notes

(1) Birks, J. B. *Photophysics of Aromatic Molecules*; Wiley-Interscience: New York, 1970.
(2) (a) Noyes, R. M. In *Progress in Reaction Kinetics*; Porter, G., Ed.; Pergamon Press: Oxford, 1961; Vol. 1. (b) Gosels, U. M. In *Progress in Reaction Kinetics*; Pergamon Press: Oxford, 1984; Vol. 13. (c) Rice, A. S. In *Comprehensive Chemical Kinetics*;

Banford, C. H., Tripper, C. F. H., Compton, R. G., Eds.; Elsevier: New York, 1985.
(3) For intermolecular excimer formation between end-labeled polymer samples, see, for example: Martinho, J. M. G.; Sienicki, K.; Blue, D.; Winnik, M. A. *J. Am. Chem. Soc.* **1988**, *110*, 7773.
(4) For intermolecular excimer formation between organic molecules, see, for example: Martinho, J. M. G.; Winnik, M. A. *J. Phys. Chem.* **1987**, *91*, 3640.
(5) For intermolecular excimer formation between organic molecules, see, for example: Klöpffer, W. In *Organic Molecular Photophysics*; Birks, J. B., Ed.; Wiley: London, 1973.
(6) For intramolecular excimer formation between end-labeled polymer samples, see, for example: Winnik, M. A.; Redpath, A. E. C.; Paton, K.; Danhelka, J. *Polymer* **1984**, *25*, 91.
(7) Wilemski, G.; Fixman, M. *J. Chem. Phys.* **1973**, *58*, 4009.
(8) Wilemski, G.; Fixman, M. *J. Chem. Phys.* **1974**, *60*, 866.
(9) Wilemski, G.; Fixman, M. *J. Chem. Phys.* **1974**, *60*, 878.
(10) Sunagawa, S.; Doi, M. *Polym. J.* **1975**, *7*, 604.
(11) Doi, M. *Chem. Phys.* **1975**, *9*, 455.
(12) Sunagawa, S.; Doi, M. *Polym. J.* **1975**, *8*, 239.
(13) Doi, M. *Chem. Phys.* **1975**, *11*, 107, 115.
(14) Szabo, A.; Schulten, K.; Schulten, Z. *J. Chem. Phys.* **1980**, *72*, 4350.
(15) Battezzati, M.; Perico, A. *J. Chem. Phys.* **1981**, *75*, 886.
(16) Perico, A.; Cuniberti, C. *J. Polym. Sci., Polym. Phys. Ed.* **1977**, *15*, 1435.
(17) (a) Noolandi, J.; Hong, K. M.; Bernard, D. A. *Macromolecules* **1984**, *17*, 2895. (b) Noolandi, J.; Bernard, D. A. *J. Math. Phys.* **1984**, *25*, 1619.
(18) Battezzati, M.; Perico, A. *J. Chem. Phys.* **1981**, *74*, 4527.
(19) Redpath, A. E. C.; Winnik, M. A. *J. Am. Chem. Soc.* **1982**, *104*, 5604.
(20) Winnik, M. A. In *Molecular Dynamics in Restricted Geometries*; Klafter, J., Drake, J. M., Eds.; Wiley: New York, 1989.
(21) Cuniberti, C.; Perico, A. *Eur. Polym. J.* **1977**, *13*, 369.
(22) See, for example: Sienicki, K.; Winnik, M. A. *J. Chem. Phys.* **1987**, *87*, 2766.
(23) Turro, N. J. *Modern Molecular Photochemistry*; Benjamin Cummings: Menlo Park, 1978.
(24) Mahanty, J.; Ninham, B. W. *Dispersion Forces*; Academic Press: London, 1976.
(25) Pecora, R.; Berne, B. J. *Dynamic Light Scattering*; Wiley: New York, 1976.
(26) Lennard-Jones, J. E.; Devonshire, A. F. *Proc. R. Soc. London* **1937**, *A163*, 53.
(27) Zwanzig, R. In *Molecular Fluids*; Balian, R., Weill, G., Eds.: Gordon and Breach: London, 1976.
(28) Kirkwood, J. G. *Recl. Trav. Chim. Pays-Bas* **1949**, *68*, 649; *J. Polym. Sci.* **1954**, *12*, 1.
(29) Liu, G. J.; Guillet, J. E. *Macromolecules* **1990**, *23*, 2969.
(30) Lui, G. J.; Guillet, J. E. *Macromolecules* **1990**, *23*, 2973.
(31) Xu, H. L. M.Sc. Dissertation, University of Toronto, 1988.